Prinprint PFC/JA-83-17

VELOCITY DIAGNOSTICS OF MILDLY RELATIVISTIC, HIGH CURRENT ELECTRON BEAMS

R.E. Shefer, Y.Z. Yin, and G. Bekefi

Plasma Fusion Center and
Research Laboratory of Electronics
Massachusetts Institute of Technology
Cambridge, MA. 02139

May 1983

VELOCITY DIAGNOSTICS OF MILDLY RELATIVISTIC, HIGH CURRENT ELECTRON BEAMS

R.E. Shefer, Y.Z. Yin,* and G. Bekefi

Department of Physics and Research Laboratory of Electronics

Massachusetts Institute of Technology

Cambridge, Massachusetts 02139

ABSTRACT

We describe two diagnostic methods for measuring the velocity of mildly relativistic, high current electron beams. The first involves a measurement of the radial electrostatic potential and of the beam current and yields the time resolved, spatially averaged axial beam velocity $v_{\parallel}$. The second requires a measurement of the beam cyclotron wavelength in the guiding magnetic field and yields the product $\gamma v_{\parallel}$, where $\gamma=\left(1-v_{\parallel}^2/c^2-v_{\perp}^2/c^2\right)^{-\frac{1}{2}}$ and $v_{\perp}$ is the transverse beam velocity. By combining the two techniques we obtain $v_{\parallel}$ and $v_{\perp}$ for a 0.4-1.2MV electron beam carrying a current of 1-2kA.

*Permanent address: Institute of Electronics, Academia Sinica, Beijing, People's Republic of China.

I. INTRODUCTION

The past ten years have seen a great deal of interest in the production of high-power millimeter and submillimeter wavelength radiation with free electron devices such as the gyrotron[1] and the free electron laser.[2] In contrast with conventional microwave tubes which typically use 1-20 keV, milliampere beams, these devices employ 50 keV-2MeV electron beams with current densities of up to tens of kiloamperes per square centimeter. In addition, their operating frequency and efficiency are extremely sensitive[3,4,5] to the electron velocity components in the beam. In this paper we discuss two velocity diagnostic techniques which may be used with high energy, high current density beams. Both diagnostics have been successfully tested on an electron beam with an energy of 400-1200 keV carrying a current of 1-2kA.

The first technique, used successfully by Avivi et al[6] on a low current beam, involves a simultaneous measurement of the beam current and radial electrostatic potential. The beam current is measured with a Rogowski coil or a current viewing resistor, and the potential is determined from the voltage across a cylindrical capacitor coaxial with the beam. These measurements allow one to determine the time resolved, spatially averaged axial streaming velocity $v_{\parallel}$ in the beam.

The second diagnostic[7] measures the electron cyclotron wavelength in a beam propagating in a uniform guiding magnetic field. This is accomplished by placing a small pinhole aperture in the path of the beam, and a moveable collector of comparable diameter downstream of the pinhole. The observed spatial periodicity of the collected current allows one to calculate the product $\gamma v_{\parallel}$ in

the beam. Here $\gamma=\left(1-v_{\parallel}^2/c^2-v_{\perp}^2/c^2\right)^{-\frac{1}{2}}$ and $v_{\perp}$ is the transverse velocity component.

We note that the first diagnostic, the capacitive velocity probe, yields information about $v_{\parallel}$ alone, whereas the cyclotron wavelength probe measures a combination $v_{\parallel}$ and $v_{\perp}$. By combining the two diagnostics, a full description of the electron beam may be obtained which has been the major aim of our experiments.

In section II we describe the experimental apparatus which provides the electron beam used for testing both diagnostics. In sections III and IV we describe the capacitive velocity probe and the cyclotron wavelength probe respectively and discuss the experimental results. In section V we combine the two sets of measurements to obtain a complete description of the velocity components in the electron beam and discuss the advantages and problems inherent in each technique.

II. EXPERIMENTAL APPARATUS

The experimental arrangement is shown in Fig. 1. A Physics International Pulserad 110A electron accelerator (1.5MV, 30kA) is used to energize a foilless field emission electron gun shown in detail in the lower portion of the figure. The electron gun consists of a graphite needle cathode 1.6mm in diameter and a concentric anode ring. The electron beam propagates in a 19mm ID evacuated drift tube and carries a current of 1-2kA. Damage patterns indicate that a large fraction of the beam current is carried in a solid core approximately 4mm in diameter. Both the electron gun and the attached drift tube are immersed in the guiding axial magnetic field of a 1 meter long pulsed solenoid. The solenoidal field may be var-

ied from 4 to 22kG and rises in 20ms. It may, therefore, be considered constant during the 30ns pulse of the electron accelerator.

The approximate locations of the velocity diagnostics in the drift tube are shown in Fig. 1. The cylindrical capacitor and Rogowski coil comprise the capacitive probe while the pinhole aperture and collector comprise the cyclotron wavelength probe. In the experiments described below, an additional aperture was placed immediately downstream of the electron gun. This aperture is a graphite cylinder 4cm long with an inner diameter of 9.53mm. The purpose of this aperture was to limit the radius of the beam thereby preventing electrons at large radii from damaging the dielectric insulator between the electrodes of the cylindrical capacitor. Furthermore, electrons striking the capactor give rise to erroneous results. We point out that the capacitor and Rogowski coil constitute a nonperturbing diagnostic, and may thus be used in conjunction with an ongoing experiment, as for example a free electron laser or gyrotron.

III. THE CAPACITIVE VELOCITY PROBE

The capacitive velocity probe is made up of a cylindrical capacitor surrounding the electron beam and a current detector. A schematic of such a system is shown in Fig. 2. When the electron beam passes through the center of the capacitor, a potential difference develops between the capacitor plates. This potential difference, $V(t)$, is equal to the integral of the radial space charge electric field of the beam, $E_r(r,t)$, from the inner (r=a) conductor to the outer (r=b) conductor of the capacitor,

$$V(t) = -\int_a^b E_r(r,t)\,dr. \qquad (1)$$

Using Gauss' law to calculate $E_r(r,t)$ we find that,

$$V(t) = -\frac{e\ell}{C}\int_0^R n(r,t)2\pi r\, dr \tag{2}$$

where $n(r,t)$ is the local electron number density at a radius r in the beam, R is the beam outer radius, and $C=2\pi\varepsilon_0\kappa\ell/\ell n(b/a)$ is the capacitance; ℓ is the length of the capacitor, and κ is the dielectric coefficient of the insulator. In this way, a measurement of $V(t)$ along with an accurate knowledge of C may be used to determine the value of the integral in Eq. (2) which is just the charge per unit length in the beam. This quantity is used along with a simultaneous measurement of the beam current $I(t)=-e\int_0^R v_{\parallel}(r,t)n(r,t)2\pi r dr$ to yield the spatially averaged axial velocity in the beam,

$$v_{\parallel}(t) = \frac{\int_0^R v_{\parallel}(r,t)n(r,t)2\pi r\, dr}{\int_0^R n(r,t)2\pi r\, dr} \tag{3a}$$

$$= \frac{\ell}{C}\frac{I(t)}{V(t)} \tag{3b}$$

The capacitor used in the experiments is composed of a stainless steel cylinder 8.9cm long placed inside the grounded drift tube which serves as the second concentric conductor. The inner cylinder is separated from the drift tube by a 2mil gap which is filled with a layer of teflon dielectric. Teflon[8] was chosen as the insulating material because it has a dielectric constant which is independent of frequency at the frequencies corresponding to the rise time of the beam pulse and because it has a high dielectric strength. Dielectric strength is important in our experiments because the electric fields between the capacitor plates are typically on the order of 200kV/cm. The teflon insulation was extended 2cm beyond the

edges of the inner conductor (see Fig. 2) in order to prevent surface flashover. The capacitance of this configuration was measured on a precision capacitance bridge to be 440pF.

The lead from the inner conductor of the capacitor is brought out through a high voltage vacuum feedthrough in the drift tube wall where it is connected to a standard 1.0kΩ carbon resistor. The RC time constant of this circuit is chosen to be more than a factor of ten longer than the duration of the electron beam pulse (30ns). This insures a proper determination of the capacitor voltage. The resistor is contained in an electrically shielded compartment adjoining the drift tube and is connected to a coaxial cable terminated in a 50Ω load. The resistor, together with the cable and load comprise a voltage divider which attenuates the signal so that it can be displayed on a fast oscilloscope (Tektronix Model 7633). Current passing through the capacitor is measured in two ways, with a Rogowski coil and with a 1mΩ current viewing resistor (CVR) connected to a graphite collector immediately downstream of the capacitor. The data presented in this paper were obtained using the latter method since we were able to obtain a more accurate calibration for the CVR.

Figures 3a and 3b show the time history of the signals on the capacitor and CVR respectively. Figure 3c shows the resulting time-resolved $v_{\parallel}(t)$ calculated from Eq. (3b) by matching the leading edges of the current and voltage signals. Note that the form of $v_{\parallel}(t)$ is qualitatively similar to the curves shown in Figs. 3a and 3b.

Measurements of the peak beam velocity $v_{\parallel}$ during the voltage pulse have been carried out for a range of values of V_0, the accel-

erating potential at the electron gun, and B_z, the uniform axial magnetic field. In the results presented below $v_{\parallel}$ is calculated from Eq. (3b) using the peaks of the current and capacitor voltage signals. In Fig. 4, $\beta_{\parallel}=v_{\parallel}/c$ is plotted as a function of $\gamma_o = 1+eV_o/m_oc^2$ for four values of B_z. Each datum point represents an average of four successive measurements. The dashed curve at the top of the figure is the speed,

$$\beta_o = v_o/c = \left(1 - \gamma_o^{-2}\right)^{\frac{1}{2}} \qquad (4)$$

which an electron would acquire by traversing the full potential difference between cathode and anode at the electron gun.

It is noteworthly that all of the values of $\beta_{\parallel}$ plotted in Fig. 4 fall well below the dashed curve which represents β_o. There are several effects which may be responsible for this difference. First, because of the strong fringing electric fields[9] at the cathode tip, the electrons acquire velocity components transverse to the axis in addition to their axial velocity $v_{\parallel}$. Secondly, the electron beam produces a radial space charge field[10,11] in the drift tube which causes the electrons to slow down. And thirdly, various plasma effects in the electron gun may prevent the beam electrons from acquiring the full accelerator energy.

IV. THE CYCLOTRON WAVELENGTH PROBE

As mentioned in section III, the electron beam may acquire transverse energy at the electron gun causing the electrons to travel in helical orbits. The cyclotron wavelength probe measures the cyclotron wavelength of beam electrons gyrating in a uniform axial magnetic field. The components of the probe are illustrated in Fig.

5. A conducting disk with a small pinhole aperture on axis is placed in the drift tube. The collector, which lies on the axis of the drift tube and moves in the z direction relative to the aperture, is the center conductor of a miniature coaxial cable. The collector diameter is comparable to the diameter of the aperture opening. Electrons whose orbits pass through the axis of the drift tube near the location of the aperture will be transmitted and will subsequently cross the axis of the drift tube at distances $z=nL$ $(n=1,2,...)$ downstream of the aperture. Here

$$L = \left(2\pi c/\Omega_o\right)\beta_{\parallel}\gamma \tag{5}$$

where $\Omega_o=eB_z/m_o$ is the nonrelativistic cyclotron frequency in the axial field B_z, $\beta_{\parallel}=v_{\parallel}/c$ is the axial velocity component and $\gamma = \left(1-\beta_{\parallel}^2-\beta_{\perp}^2\right)^{-\frac{1}{2}}$ is the total relativistic factor of the electron. The collector current is therefore modulated in z with a spatial periodicity equal to the cyclotron wavelength L.

In the experiments, the pinhole aperture is located approximately 40cm downstream of the electron gun. The material comprising the aperture disk must withstand repetitive pulses in which the beam typically deposits $1kJ/cm^2$. It must also be thick enough to prevent electrons from passing through it. Dense Poco® graphite or molybdenum prove to be satisfactory materials. Disk thicknesses of 0.75, 2.0, and 2.5mm are used with aperture diameters of 0.5 to 1.5mm. All disks are made from graphite except the 0.75mm thick disk which is made from molybdenum. The collector is the center conductor (1.0mm diameter) of a rigid coaxial cable connected to ground through a 1mΩ low inductance current viewing resistor. The voltage across this resistor is displayed on a fast oscilloscope. Measurements are made on a shot-to-shot basis by moving the collector away from the aperture in 1, 2, or 3mm steps. The current incident on the aper-

ture is 1-2kA. The peak current measured on the collector side of the aperture is typically 10-50A.

Measurements of I(z) obtained at the same electron gun voltage and three values of B_z are shown in Fig. 6. In each case at least two periods of the current modulation are measured. For a beam in which all electrons have the same value of $v_\parallel$ and for an ideal aperture and collector we would expect the collector current to look like a set of equally spaced infinitesimally narrow peaks of equal amplitude. If the beam contains a spread in $v_\parallel$, the first peak will be broadened and each subsequent peak will be further broadened due to the loss of phase coherence of the orbits of electrons with different values of $v_\parallel$ as they propagate in the z direction. This broadening will be accompanied by a decrease in peak amplitude with z since the total number of electrons behind the aperture is conserved. This behavior is clearly demonstrated in Fig. 6 where the peaks progressively broaden and decrease in amplitude with increasing z. We believe that a detailed analysis of this behavior could be used to estimate the beam "temperature". However, such an analysis has not yet been made.

Figure 7 summarizes a set of measurements carried out at five values of B_z between 5 and 12kG. These data were obtained with an electron gun voltage V_0=680kV. We find that the modulation periodicity L varies linearly with B_z^{-1}. Here L is the distance between peaks or valleys in the collected current and represents an average cyclotron wavelength in the beam. This average is really a spatial average across the beam radius since electrons with guiding centers at any radial position may be transmitted through the aperture so long

as their orbits pass through the axis of the drift tube. The linear variation of L with B_z^{-1} is predicted by Eq. (5) for a beam in which the product $\gamma\beta_{\parallel}$ is independent of B_z.

Figure 8 shows the effect of varying the accelerating potential at the electron gun on the quantity $\gamma\beta_{\parallel}$ calculated from Eq. (5). These values of $\gamma\beta_{\parallel}$ represent an average over the beam cross-section. As expected, $\gamma\beta_{\parallel}$ increases monotonically with increasing γ_0.

In order to completely characterize the beam a knowledge of the total beam relativistic factor $\gamma=\left(1-\beta_{\parallel}^2-\beta_{\perp}^2\right)^{-\frac{1}{2}}$ or an independent measurement of $\beta_{\parallel}$ is necessary. In the following section we show how the results of this diagnostic and the capacitive velocity probe described earlier may be combined to yield values for $\beta_{\parallel}$ and $\beta_{\perp}$. We point out, however, that in low current density beams γ is well-known ($\gamma=\gamma_0$) and the cyclotron wavelength probe alone may be used to determine both the average streaming velocity $\beta_{\parallel}$ and the average transverse velocity $\beta_{\perp}$,

$$\beta_{\parallel} = \frac{L}{\gamma_0}\frac{\Omega_0}{2\pi c} \tag{6a}$$

$$\beta_{\perp} = \left[1 - \beta_{\parallel}^2 - \frac{1}{\gamma_0^2}\right]^{\frac{1}{2}} \tag{6b}$$

from a measurement of the cyclotron wavelength L and the guiding magnetic field B_z.

V. DISCUSSION

Measurements carried out with the capacitive velocity probe and the cyclotron wavelength probe may be combined to yield information about both the streaming velocity $v_{\parallel}$ and the transverse velocity $v_{\perp}$ in the electron beam. This is done in the following way: $\beta_{\parallel}$ is measured with the capacitive probe and combined with a measurement of

$\gamma\beta_{\parallel}$ from the cyclotron wavelength probe. The values of γ and $\beta_{\perp}/\beta_{\parallel}$ are then calculated. These quantities, plotted as a function of γ_o in Fig. 9, were obtained by using the measured values of $\beta_{\parallel}$ from Fig. 4 along with the measured values of $\gamma\beta_{\parallel}$ from Fig. 8.

We see in the lower portion of Fig. 9 that γ increases monotonically with γ_o and that the values of γ plotted fall slightly below (<8%) the values of γ_o. The corresponding values of $\beta_{\perp}/\beta_{\parallel}$, plotted in the upper portion of the figure, range from 0.60 to 0.76.

In the paragraphs below we discuss three possible sources of error inherent in these diagnostic techniques and their effect on the data plotted in Fig. 9. These are (a) systematic errors associated with the direct measurement of beam parameters, (b) space charge effects and (c) errors resulting from the "averaging" of $\beta_{\parallel}$ and $\gamma\beta_{\parallel}$ inherent in the two diagnostics.

a) The capacitive velocity probe technique involves measurements of V(t) and I(t) as well as a knowledge of the capacitance C. While we were able to measure C to high accuracy (1%) we note that small errors in the measurement of V(t) and I(t) lead to considerable errors in the values of $\beta_{\perp}/\beta_{\parallel}$ obtained when the results of the two dianostics are combined. For example, increasing the values of $\beta_{\parallel}$ plotted in Fig. 4 by 3% results in a decrease in $\beta_{\perp}/\beta_{\parallel}$ by 12-15% over the values plotted in Fig. 9. An underestimate of $\beta_{\parallel}$ in our system would most likely result from an underestimate of the beam current as measured by the CVR. In a short pulse, high current density beam such as ours, plasma formation, secondary emission and reflection of primary electrons from the collector surface[12] as well as finite inductance effects in the collector-CVR system may be important.

We have not studied these effects in our experiments.

We point out that the measurements carried out with the cyclotron wavelength probe are less prone to errors of this sort. This is because this technique involves only a knowledge of the axial magnetic field and the axial position of the current collector, both of which may easily be determined to high accuracy.

b) An electron beam propagating in a conducting pipe shares its total energy between the electron kinetic energies and the space charge electric fields in the pipe.[10,11] In the cyclotron wavelength probe approximately 97% of the beam electrons are collected at the aperture disk. This results in a sharp drop in the space charge field energy downstream of the aperture with a corresponding increase in the axial velocity of the transmitted electrons. The value of $\gamma\beta_{\parallel}$ measured downstream of the aperture may therefore be higher than the upstream value far from the aperture. This effect will result in an overestimate of γ, and therefore $\beta_{\perp}/\beta_{\parallel}$, when the data from this diagnostic is combined with measurements of $\beta_{\parallel}$ from the capacitive velocity probe.

c) The capacitive velocity probe and the cyclotron wavelength probe yield spatially averaged values of the quantities $\beta_{\parallel}$ and $\gamma\beta_{\parallel}$ respectively. If these averages are carried out over different populations of electrons, systematic errors may result when measurements from both probes are combined, as in Fig. 9.

The capacitive velocity probe yields a weighted average of $\beta_{\parallel}=v_{\parallel}/c$ over the entire beam cross-section, as given by Eq. (3a). The cyclotron wavelength probe only admits electrons whose orbits cross the axis of the drift tube. And, an additional restriction on the orbits of these transmitted electrons

is imposed by the admittance angle of the aperture. That is, if the aperture disk material is completely opaque to the incident electrons, the aperture will only admit electrons with $\beta_\perp/\beta_\parallel$ smaller than D/W where D is the aperture diameter and W is the thickness of the aperture disk. Both of these effects single out a certain population of electrons, and may result in errors in γ and $\beta_\perp/\beta_\parallel$ when the two diagnostics are combined. In practice, the finite electron range in the aperture disk material and the fact that the edges of the aperture are not sharp make the restriction on the maximum value of $\beta_\perp/\beta_\parallel$ less severe. Due to these considerations, a quantitative estimate of the effective value of D/W is not readily made.

In summary, two velocity diagnostic techniques have been used for the first time with intense, mildly relativistic electron beams. These diagnostics have yielded time-resolved measurements of the average axial streaming velocity in the beam as well as measurements of the total beam energy and the average transverse velocity. We believe that a high degree of accuracy can be achieved in the determination of the average streaming velocity $v_\parallel$ and of the total beam energy γ. However, the determination of the average transverse velocity $v_\perp$ is made less accurate by the fact that it is very sensitive to errors in $v_\parallel$ and $\gamma v_\parallel$.

ACKNOWLEDGMENTS

This work was supported in part by the Air Force Office of Scientific Research, in part by the Department of the Air Force Aeronautical Systems Division (AFSC), and in part by the National Science Foundation.

REFERENCES

1. J.L. Hirshfield and V.L. Granatstein, Comments Plasma Phys. Cont. Fusion 3, 87 (1977) and references therein.

2. P.A. Sprangle, R.A. Smith, and V.L. Granatstein in "Infrared and Submillimeter Waves", K. Button editor (Academic Press, N.Y. 1979) Vol. 1, page 279 and references therein.

3. N.M. Kroll and W.A. McMullin, Phys. Rev. A17, 300 (1978).

4. R.H. Jackson, S.H. Gold, R.K. Parker, H.P. Freund, P.C. Efthimion, V.L. Granatstein, M. Herndon, A.K. Kinkead, J.E. Kosakowski, and T.J.T. Kwan, IEEE J. Quantum Electronics QE-19, 346 (1983).

5. C.W. Roberson, J.A. Pasour, F. Mako, R. Lucey, and P.A. Sprangle, Memorandum Report No. 5013 (1983), Naval Research Laboratory, Washington, DC.

6. P. Avivi, C. Cohen, and L. Friedland, Bull. Am. Phys. Soc. 27, 1092, (1982).

7. J.M. Buzzi (private communication).

8. W.B. Westphal and A. Sils, "Dielectric Constant and Loss Data", Air Force Materials Laboratory Air Force Systems Command, Wright-Patterson Air Force Base, Ohio Report No AFML-TR-72-39 (1972) pp. 173, 174, 222. Mylar proved to be unsatisfactory because of the large variation of κ with frequency.

9. R.E. Shefer and G. Bekefi, Appl. Phys. Letters 37, 901 (1980).

10. J.R. Thompson and M.L. Sloan, Phys. Fluids 21, 2032 (1978).

11. L.E. Thode, B.B. Godfrey, and W.R. Shanahan, Phys. Fluids 22, 747 (1979).

12. T.P. Starke, Rev. Sci, Instrum. 51, 1473 (1980); the graphite current collector was made in the shape of an inverted cone in order to reduce errors due to secondary and reflected primary electrons.

FIGURE CAPTIONS

Fig. 1. Experimental arrangement showing the location of the capacitive velocity probe and cyclotron wavelength probe. A detail of the electron gun is shown in the lower portion of the figure.

Fig. 2. Schematic of the capacitive velocity probe.

Fig. 3. Time history of (a) the voltage on the capacitor, (b) the beam current and (c) $v_{\parallel}(t)$ calculated from Eq. 3b, on a single shot.

Fig. 4. $\beta_{\parallel}=v_{\parallel}/c$ as a function of γ_o measured with the capacitive velocity probe for four values of B_z. The dashed curve represents the values of $\beta_o=\left(1 - \gamma_o^{-2}\right)^{\frac{1}{2}}$

Fig. 5. Schematic of the cyclotron wavelength probe.

Fig. 6. Measured current as a function of distance z behind the midplane of the aperture disk (z=0) for V_o=680kV.

Fig. 7. Measured current modulation periodicity L as a function of B_z^{-1} for V_o=680kV.

Fig. 8. $\gamma\beta_{\parallel}=L\Omega_o/2\pi c$ calculated from the measured values of L and $\Omega_o=eB_z/m_o$ as a function of $\gamma_o=1+eV_o/m_oc$ where V_o is the accelerating potential at the electron gun.

Fig. 9. γ and $\beta_{\perp}/\beta_{\parallel}$ as a function of $\gamma_o=1+eV_o/m_oc$ obtained by combining the measurements of $\beta_{\parallel}$ from Fig. 4 with the measured values of $\gamma\beta_{\parallel}$ from Fig. 8.

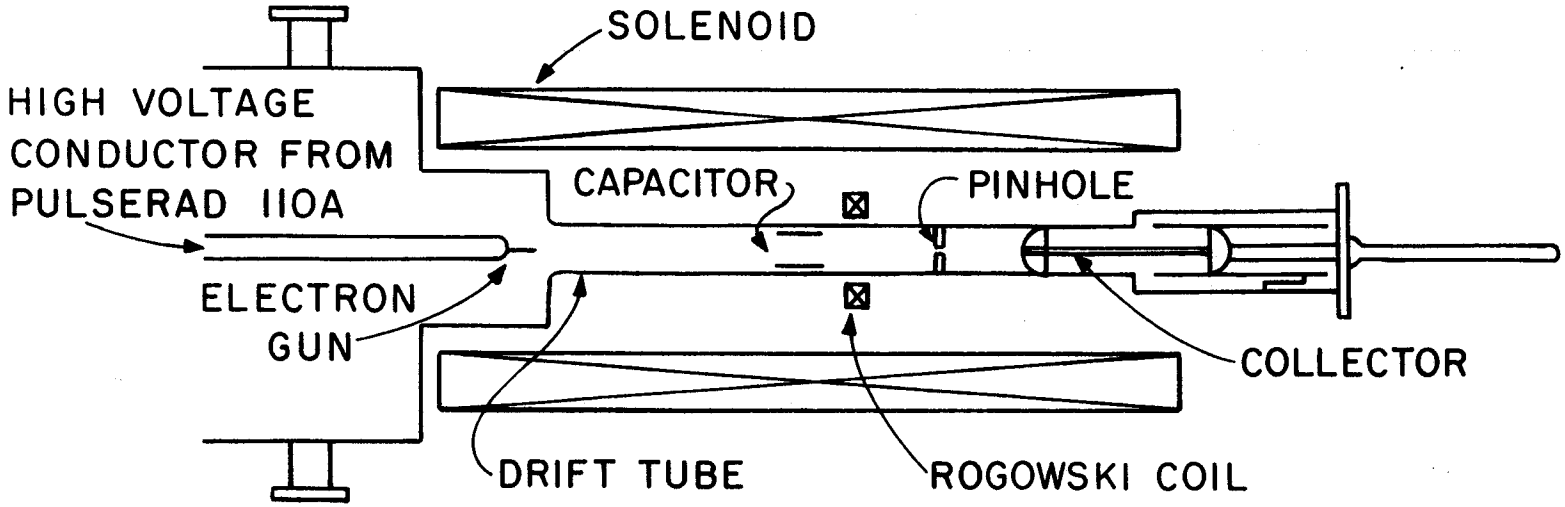

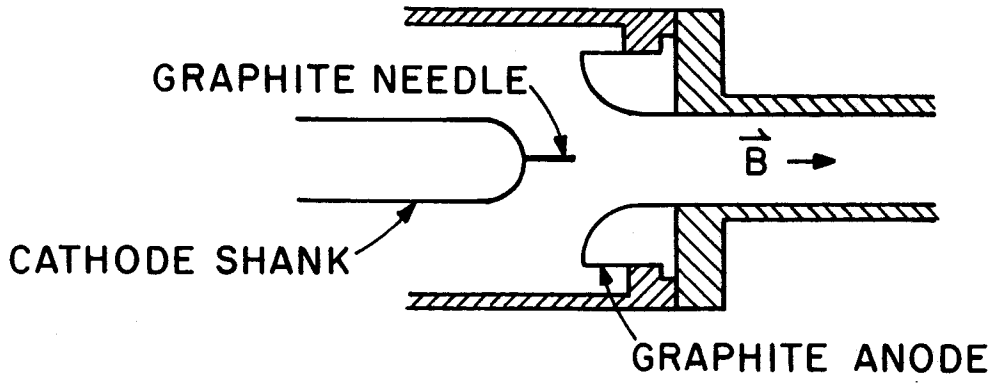

Fig. 1
Shefer, Yin, Bekefi

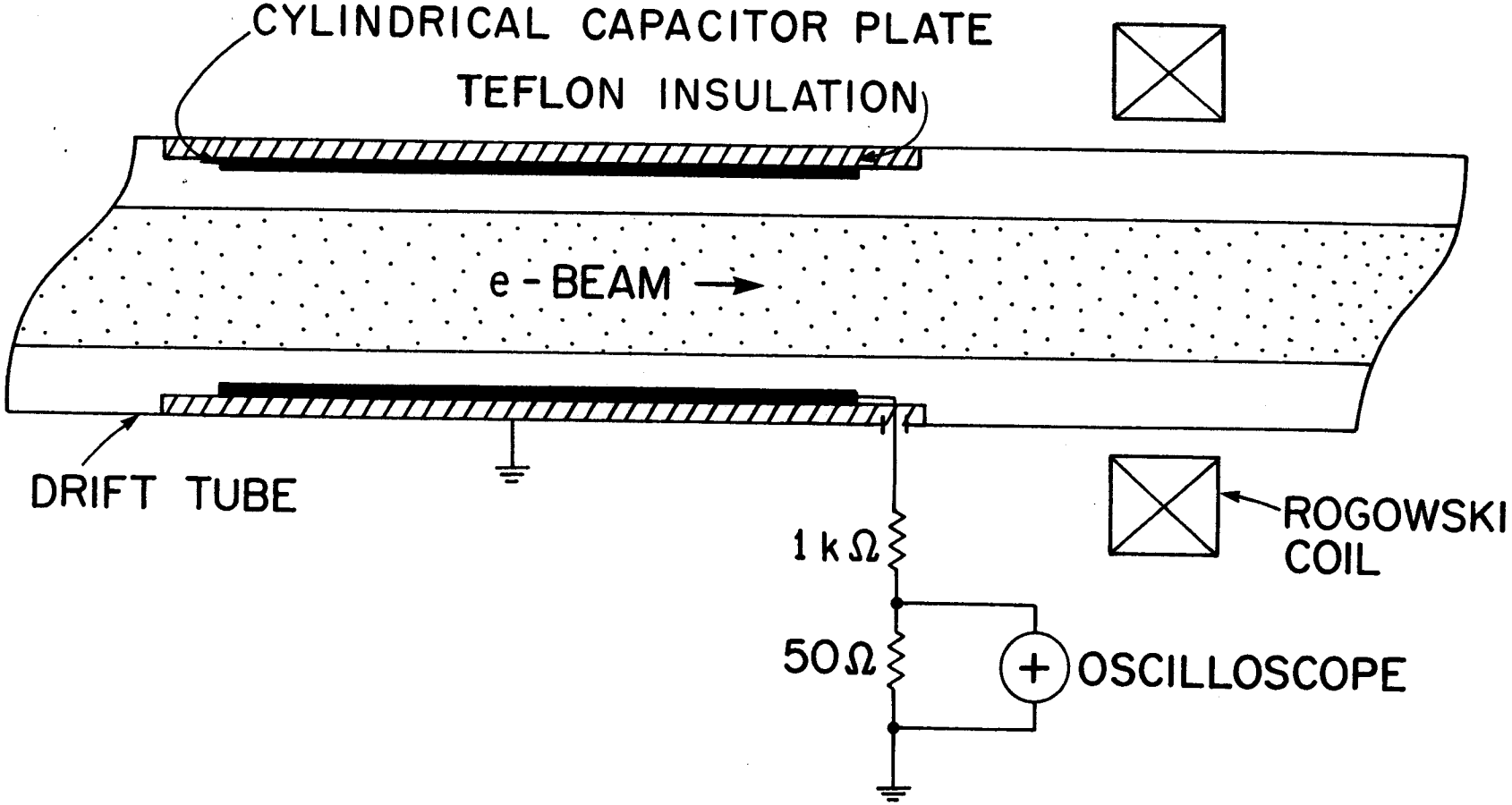

Fig. 2
Shefer, Yin, Bekefi

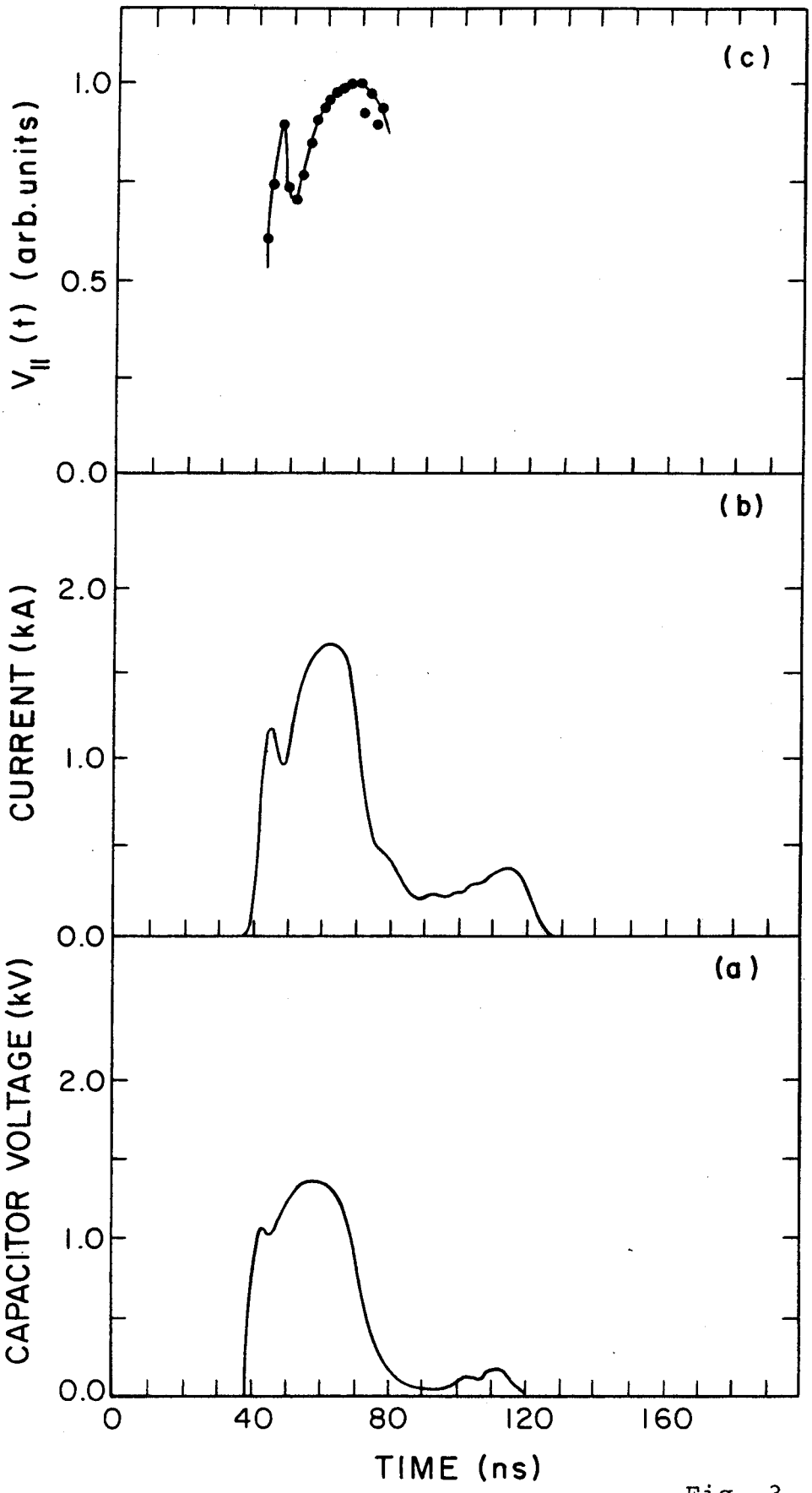

Fig. 3
Shefer, Yin, Bekefi

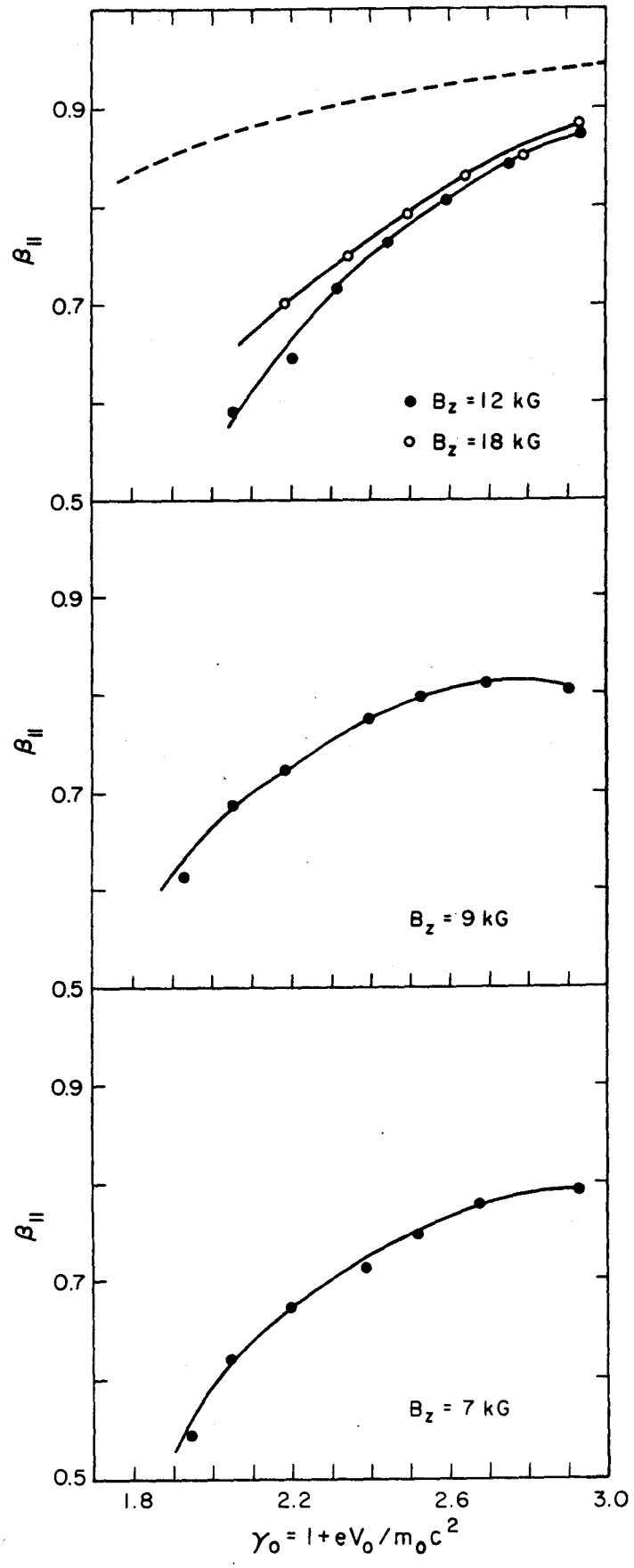

Fig. 4
Shefer, Yin, Bekefi

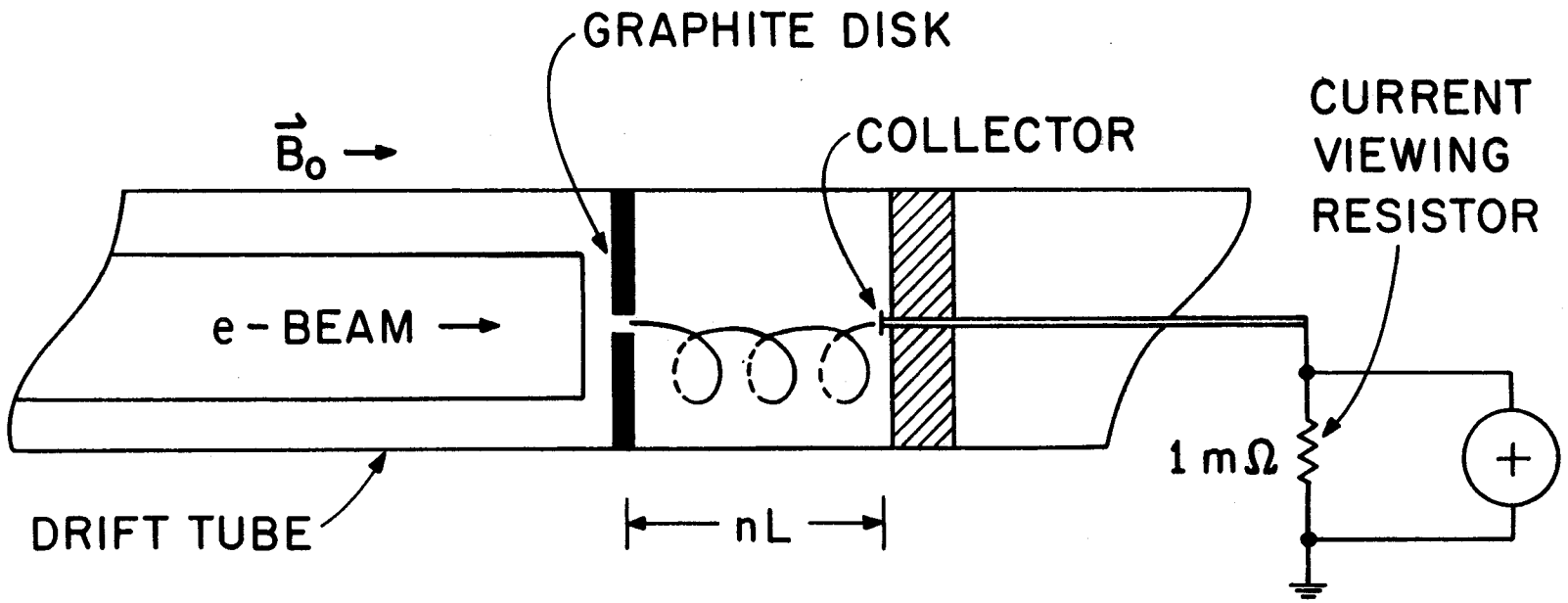

Fig. 5
Shefer, Yin, Bekefi

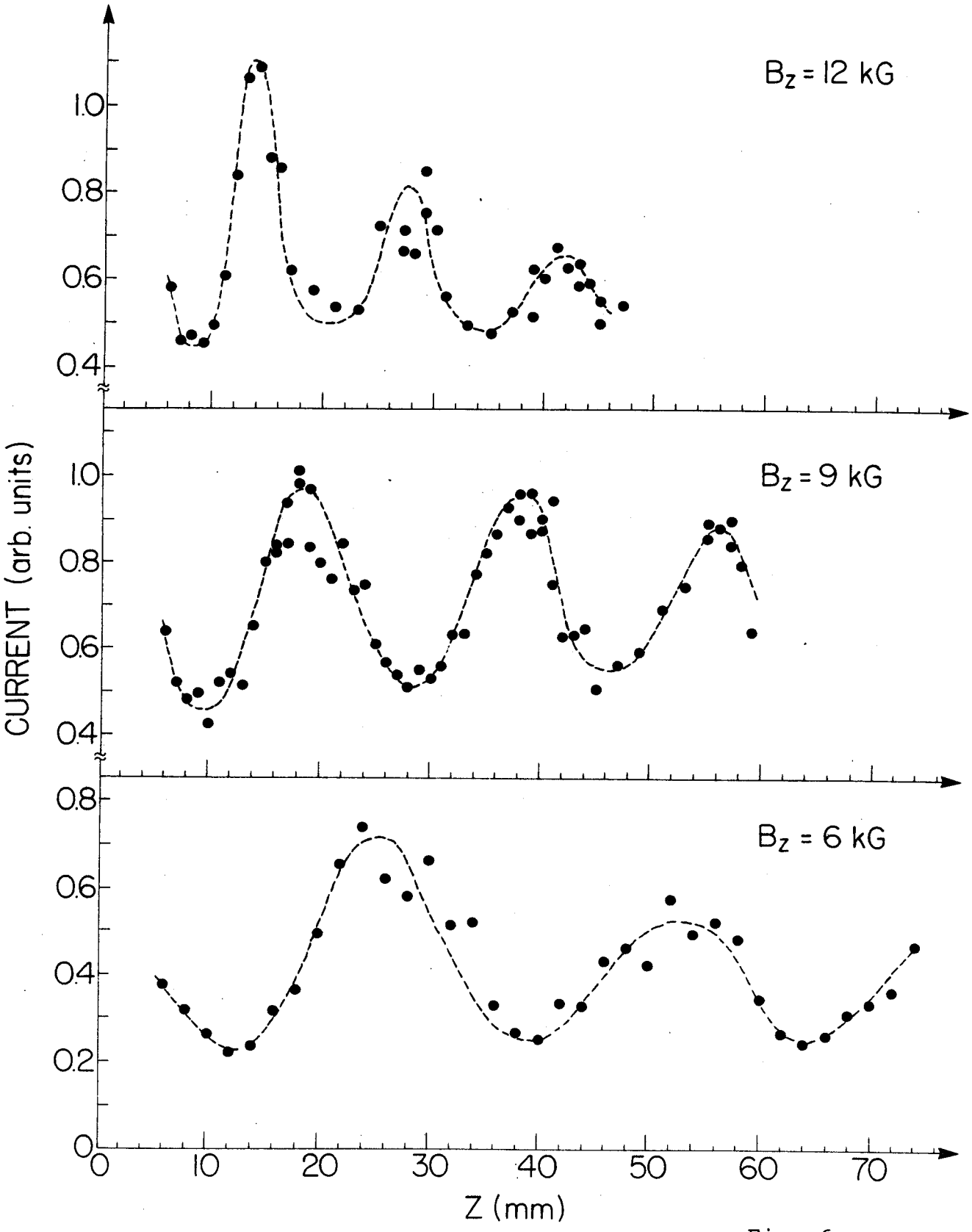

Fig. 6
Shefer, Yin, Bekefi

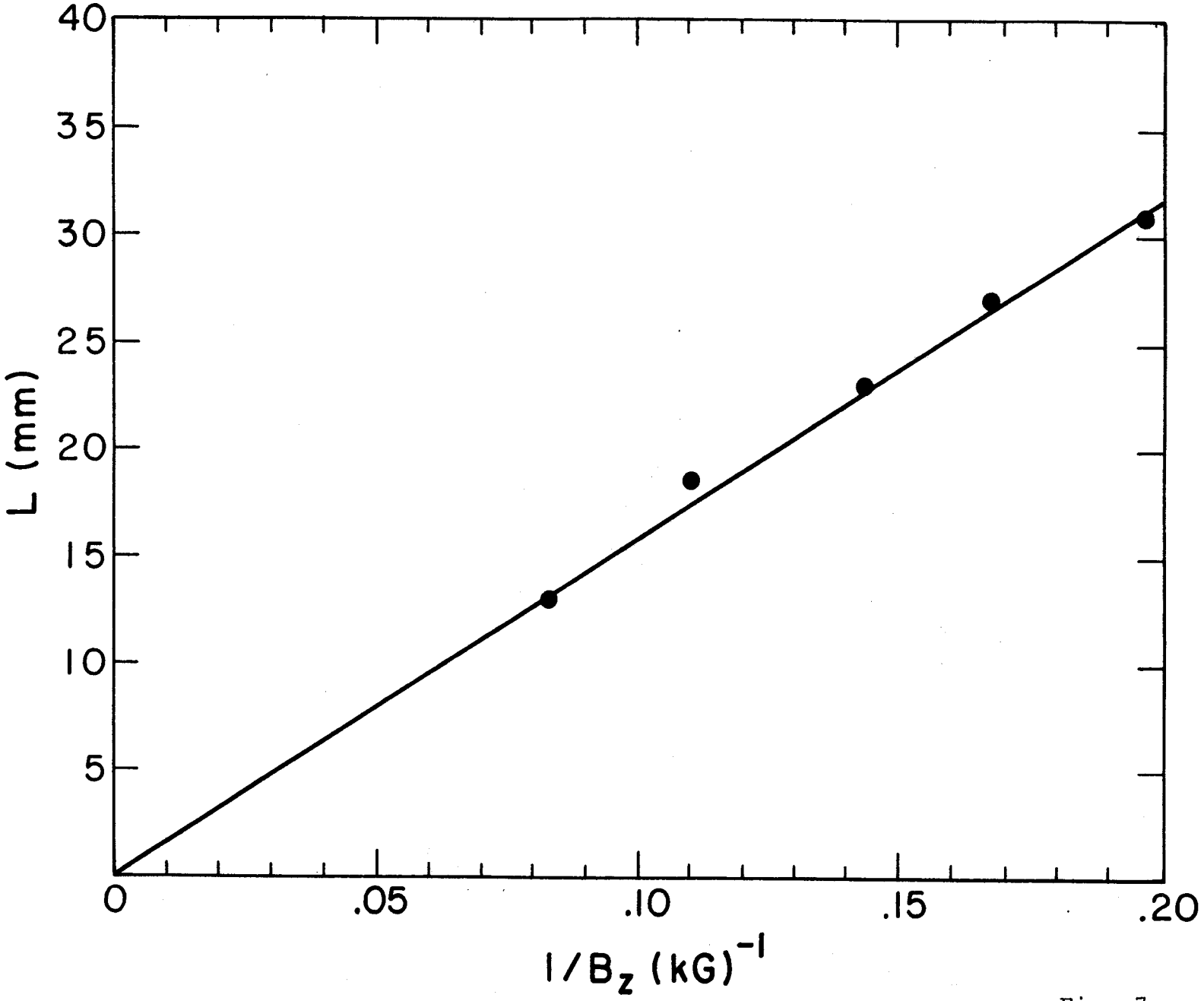

Fig. 7
Shefer, Yin, Bekefi

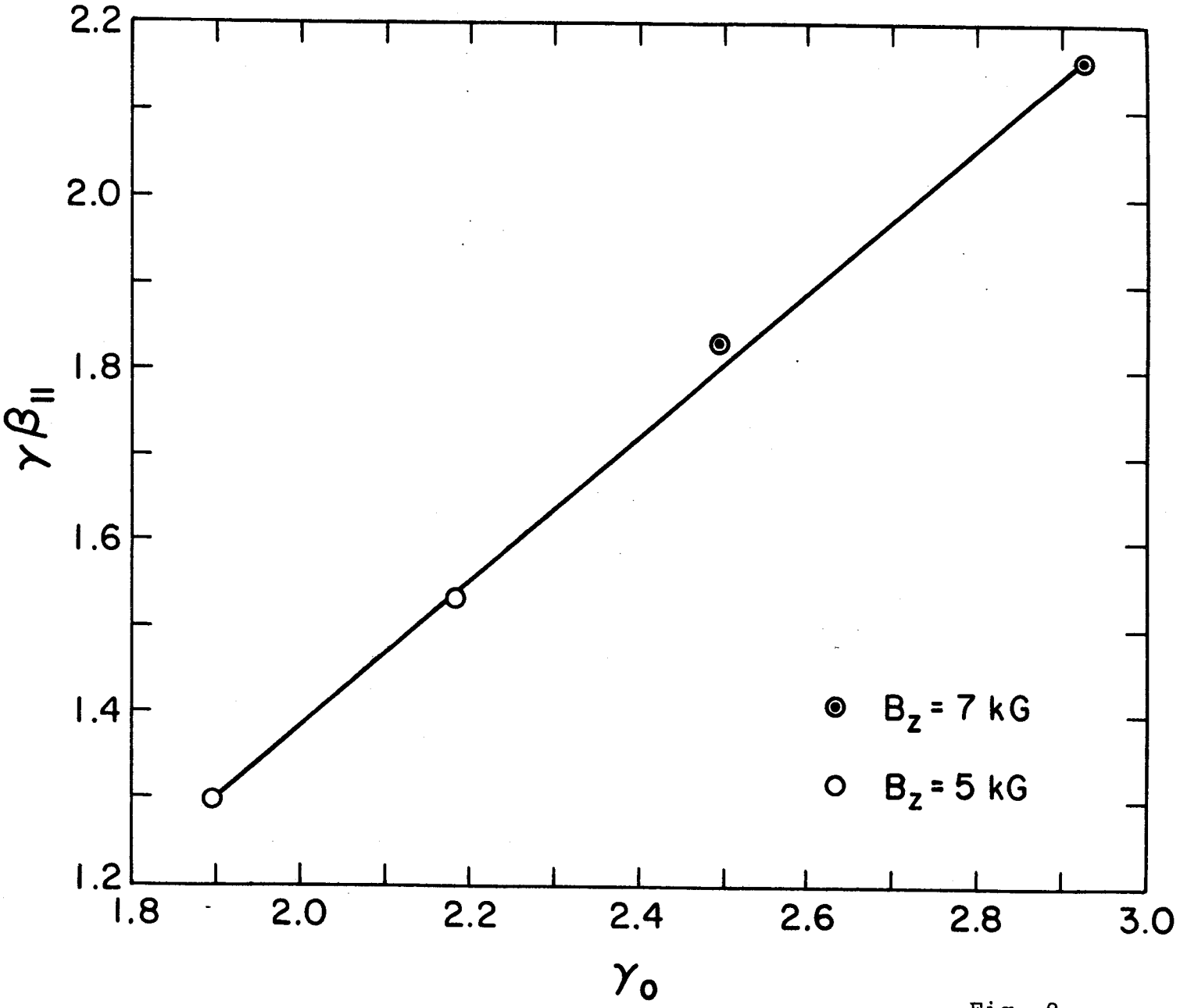

Fig. 8
Shefer, Yin, Bekefi

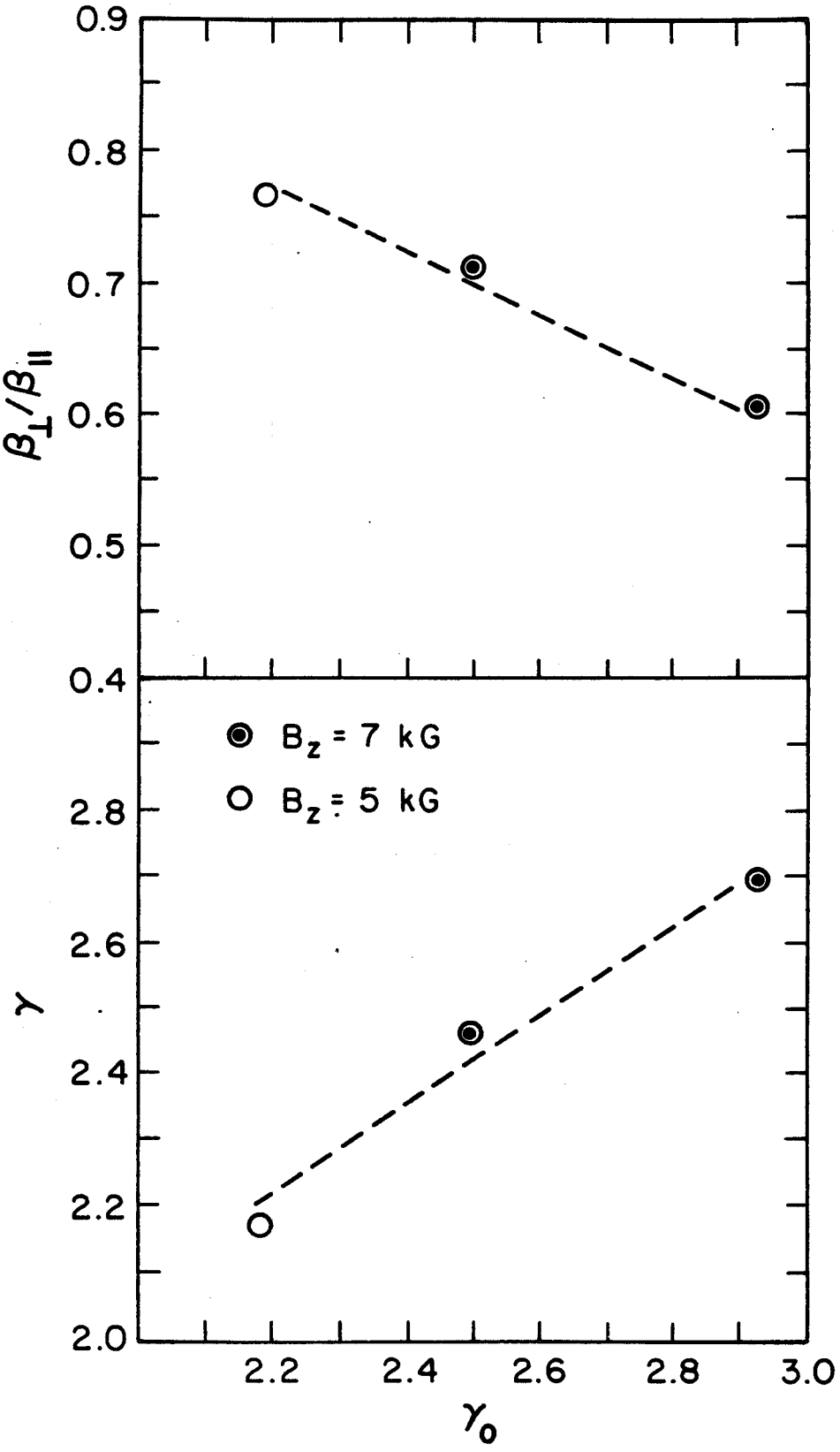

Fig. 9
Shefer, Yin, Bekefi